Analysis of the interaction of CO_2 with Na, K, and Ca-exchanged Mordenite. An infrared spectroscopic study

Aline Villarreal, Perla Castillo-Villalón and Jorge Ramírez*

UNICAT, Dpto. Ingeniería Química, Facultad de Química, Universidad Nacional Autónoma de México, Ciudad Universitaria, 04510, México, D.F., México.
* Autor de correspondencia: Jorge Ramírez
Tel: (+52) 55 5622 5349. E-mail: jrs@unam.mx

Abstract. To enquire on the CO_2 capture on solid adsorbents, the interactions of CO_2 with mordenite exchanged with Na, K, and Ca were analyzed using FTIR spectroscopy. The results reveal that physisorbed CO_2 and different carbonate species are present on the zeolite surface. At high CO_2 concentration, the cation polarizing power determines the type of carbonates formed: mainly bidentate carbonates on Ca-mordenite; bi and polydentate carbonates on Na-mordenite; polydentate carbonates on K-mordenite. At low CO_2 (10^{-4} Torr), mostly bidentate carbonates are formed. Pre-adsorbed water produces bicarbonates and decreases CO_2 adsorption.
Keywords: CO_2 capture; (Na, K, Ca)-Mordenite; chemisorbed carbonates; IR spectroscopy; interaction CO_2-mordenite.

Resumen. Para investigar sobre la captura de CO_2 en adsorbentes sólidos, se analizaron las especies formadas en la interacción de CO_2 con mordenita intercambiada con Na, K y Ca. Los resultados muestran CO_2 fisisorbido y diferentes especies de carbonatos en la superficie de la zeolita. A alta concentración de CO_2, el poder polarizante del catión determina el tipo de carbonatos formados: bidentados en Ca-mordenita, bi y polidentados en Na-mordenita y polidentados en K-mordenita. A baja concentración de CO_2 (10^{-4} Torr), se forman carbonatos bidentados. Agua preadsorbida produce bicarbonatos y disminuye la adsorción de CO_2.
Palabras clave: Captura de CO_2; (Na, K, Ca)-Mordenita; carbonatos quimisorbidos; espectroscopia infrarroja IR; interacción CO_2-mordenita.

Introduction

Biogas is an important source of renewable energy, produced by the anaerobic fermentation of biomass by methanogenic bacteria [1,2]. Typically, biogas contains methane and carbon dioxide along with other contaminants [3]. The presence of CO_2 lowers the specific heat capacity of biogas and limits its utilization [4,5]. One of the strategies to reduce the amount of CO_2 in biogas is to separate it selectively from methane using feasible adsorbents such as zeolites [6,7] or activated carbon [8,9]. According to the literature, CO_2 is mainly physisorbed and also chemisorbed on zeolites [6,10,11]. The chemisorption of CO_2 on zeolites can produce several types of carbonates, some of them very stable [10,12,13].

The formation of carbonate species inside the cavities of the zeolites is small compared to the physisorbed CO_2. However, the presence of carbonates on the surface can hinder the physisorption of CO_2, lowering the adsorption capacity of the zeolite [14]. Therefore, careful control of the carbonate formation during the CO_2 adsorption process is necessary for the efficient performance of zeolites i.e., in pressure (or temperature) swing adsorption processes [15].

The adsorption of carbon dioxide on zeolites is mainly affected by the structure of the cavity, the amount and type of exchangeable cations [13,16–18], and the presence of other molecules such as water[14].

Gallei and Stumpf [10] proposed a mechanism for carbonate formation during the adsorption of CO_2 in Na- and Ni-exchanged Y zeolite. According to their proposal, to produce monodentate carbonate, the first step is the polarization of the CO_2 molecule by the exchanged cation. They observed that the formation of carbonates on zeolites can be largely influenced by the polarizing power of the cation.

The polarizing power of a cation is calculated as the cation charge divided by the square of the ionic radius (Z^+/r_{ionic}^2). Small cations with high charge have large polarizing power [19]. In the case of cations inside the zeolite framework, the polarizing power decreases due to their interaction with the framework oxygens, and can also be affected by the presence of other molecules such as water [20]. Since the cations can be in different sites of the zeolite framework, not all them have the same polarizing power and consequently the strength of the interaction with CO_2 is different.

The effect of the presence of water molecules that interact strongly with the exchanged cations is not yet completely understood. For the adsorption of CO_2 in faujasite some authors observed a decrease in the global amount of adsorbed CO_2 and concluded that water can delay [10] or impede the formation of carbonates [10,21,22]. However, other reports on the CO_2 adsorption on 13 X and 5A zeolites indicate that water can increase the amount of adsorbed CO_2 due to the formation of bicarbonate species [23].

Almost all the research on the effect of the polarizing power of cations in the formation of carbonates in zeolites has been performed with large pore zeolites and little information exists explaining this effect for medium pore zeolites where molecular sieving effects are important, such as in the case of mordenite.

Mordenite (MOR) has interesting properties for CO_2 selective adsorption due to its channel structure, with main channels that allow the entrance of molecules up to 6.7 Å, connected by side pockets of smaller diameter (3.9 Å) [24], in addition to its affinity towards polar molecules, wide availability and low cost [25].

The aim of this work is to investigate the effect of exchanging mordenite with different cations (Na, K, Ca) on the type of carbonates formed during the adsorption of carbon dioxide, with and without the presence of adsorbed water. For this purpose, we contacted Na^+, K^+ and Ca^{2+} exchanged mordenite with CO_2 in a high vacuum line and followed, by *in situ* infrared spectroscopy, the formation of surface carbonates during the adsorption and desorption of CO_2.

2. Experimental

2.1 Exchanged zeolites preparation

Calcium, sodium and potassium mordenite $((Ca, Na_2, K_2) Al_2Si_{10}O_{24} \cdot 7H_2O)$, called hereafter Ca-MOR, Na-MOR and K-MOR, were prepared by cationic exchange, using Na-MOR (Zeolyst) as starting material. For the cationic exchange, 10 mL of 1 M solution of $CaCl_2$ (Baker, 94.65%) or KCl (Mallinckrodt, 99%) were added to one gram of Na-MOR powder. The suspension was stirred for 7 h at 353.15 K and then centrifuged. The powder was washed with water several times (~6 times) to eliminate the remaining Cl^- ions (detected with a pH sensor).

To prepare Na-H-MOR, the cationic exchange was performed using a 0.01 M HNO_3 solution (Aldrich, 70%). The suspension was stirred at room temperature for 7 h, centrifuged and washed.

The zeolites were dried overnight at 393 K, treated in a dry air flow (50 mL/g min) at 363 K for 1h (heating ramp 1K/min), and then at 723 K for 2 h (heating ramp 5 K/min). The samples were stored in ambient conditions.

2.2 Characterization

The composition of the samples (Na, K, Ca, Si, Al, and O) was determined by SEM-EDX with a JEOL JSM-5900-LV microscope coupled with microanalysis Oxford ISIS.

The textural properties of the zeolites were calculated with the N_2 adsorption-desorption isotherms obtained with a Micromeritics Tristar 3000 after evacuating the samples overnight at 573 K. The microporous volume was determined using the t-plot method.

The X-ray diffractograms were registered on a D8 Advance Davinci X-ray diffractometer (Cu Kα, λ=0.154 nm) in the scanning range from 0 to 80° (2θ), with a step size of 0.02°/min.

2.3 FT-IR analysis of CO_2 adsorption

For the IR analysis, the zeolites were pressed into self-supported discs of about 2 cm of diameter (~25 mg). The prepared wafer was introduced into a cell with KBr windows that allows treating the samples under heat and vacuum. For activation, the zeolite wafer was outgassed in vacuum (1.4×10^{-4} Torr) at 673 K for 1 h, and cooled down to room temperature.

After activation, the sample was contacted at room temperature with increasing measured amounts (~26, 66, 100, 110 and 130 µmol) of CO_2 (99.99% pure, INFRA). The IR spectra were recorded after each CO_2 addition every 5 min during 30 min. Following the CO_2 adsorption, the cell was outgassed at room temperature for 30 min. IR spectra were also collected at the beginning and at the end of the evacuation period. The sample was then heated in vacuum to 673 K and a final spectrum was taken.

The IR spectra were recorded in a FT-IR Nicolet 380 spectrometer (DTGS detector) with a 4 cm^{-1} resolution.

3. Results and Discussion

The following sections will discuss the characteristics of the prepared zeolites: Na-MOR, Na-H-MOR, K-MOR and Ca-MOR and the IR study of the different species of carbonates produced during adsorption and desorption of CO_2, in the absence and presence of water.

3.1 Characteristics of exchanged zeolites

The prepared samples were characterized by SEM-EDS to determine their chemical composition (results in Table 1). The Na/Al ratio in Na-MOR is 0.7, close to reported values for similar materials [26].The real exchange capacity of alkaline and alkaline earth cations in mordenite is often below the maximum exchange capacity, due to the low mobility of cations in the side pockets [26]. In accordance, the Ca/Al ratio in Ca-MOR is 0.44. However, the K/Al ratio is 1.08, most likely due to a better affinity of mordenite towards K [27]. In the partially exchanged Na-H-MOR, only half of the electronically deficient sites are neutralized by Na. Regarding the Si/Al ratio, all zeolites have similar values (~5.6), except for K-MOR, where the Si/Al ratio is slightly lower.

Table 1. Chemical composition and textural properties of zeolites

Sample	Na	K	Ca	Cation/Al	Si/Al	*Micropore volume (cm^3/g)
	Atomic %					
Na-MOR	4.3	0.1	0	0.70	5.6	0.19
Na-H-MOR	2.5	0	0	0.36	5.5	0.15
K-MOR	0.3	6.7	0	1.03	5.0	0.13
Ca-MOR	0.4	0.3	2.9	0.44	5.5	0.12

* Micropores with diameters smaller than 8 Å

The XRD diffractograms of the samples are displayed in Fig. 1. The XRD of Na-MOR is consistent with the crystallographic data of mordenite (JCPDS 29-1257). All the other samples have similar diffractograms to that of Na-MOR, indicating that the ion-exchange procedure did not destroy or change the framework of the zeolite.

The samples were also characterized by N_2 adsorption (see Table 1). The shapes of the N_2 adsorption isotherms (Fig. 2) are typical of microporous materials with mesopores. Since X-ray diffractograms showed that all prepared samples are fully crystalline materials, the mesopores can be explained by intraparticular space.

The isotherms were analyzed using the t-plot method [28,29] to obtain the micropore volume (Table 1). The K and Ca exchanged mordenites show a reduced pore volume that can be explained with the position of these cations inside the mordenite channels. According to the literature [20,27,30], K^+ and Ca^{2+} are placed at two positions in the gate of the side pockets blocking the entrance to these channels. These results indicate that the ion-exchanged mordenites retained the framework characteristics of the starting Na-MOR zeolite.
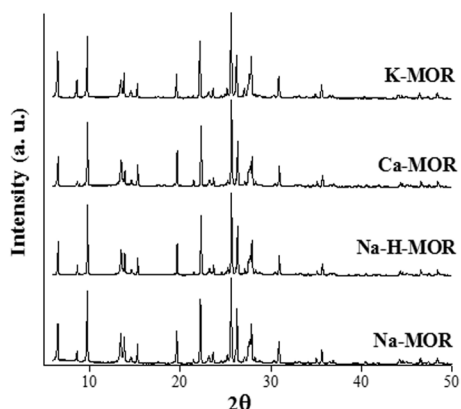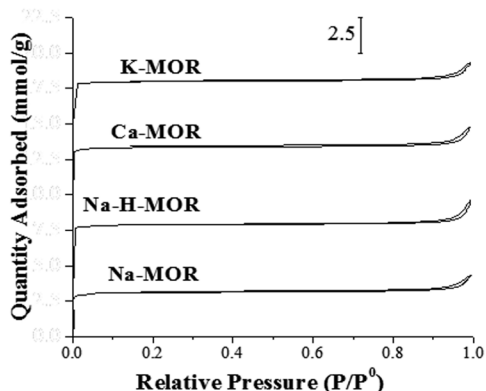
3.2 Formation of carbonates during the adsorption of CO_2 on Na-MOR

CO_2 adsorption in zeolites produce physisorbed CO_2 and carbonates [6,10,14]. Infrared spectroscopy has revealed that several species can be formed, such as mono, bi, and polydentate carbonates, along with bicarbonate [10,31,32]. The type of carbonate formed is a consequence of the type of zeolite framework and of the polarizing power of the exchanged cation [18].

The presence of water in CO_2 adsorption is also important since it modifies the polarization power of the cations at the interior of the framework and can prevent the adsorption of the CO_2 molecule.

To investigate the effect of the presence of water in Na-MOR in the formation of carbonates, the zeolite was activated at 473 or 673 K. These temperatures are below and above 573 K, where the main step of dehydration of the mordenite occurs [27,33,34].

Fig. 3 displays the spectra of Na-MOR exposed to increasing amounts of CO_2 for 30 min. Several spectra were taken (every 5 min) after the initial contact with CO_2. The absorbance of the spectra grows in the first minutes of the contact between the gas and the solid and then reaches a plateau.

The bands at 1705, 1682, 1654, 1634 and 1618 cm^{-1} along with the bands at 1361 and 1335 cm^{-1} can be attributed to different species of carbonates. However, the assignation of each band to a specific type of carbonate is not straightforward. The spectra also show a band at 1380 cm^{-1}, assigned to physisorbed CO_2. In general, the absorbance of the bands increases with each addition of CO_2; in the case of the bands at 1670-1550 cm^{-1}, the band at 1618 cm^{-1} becomes predominant.

It is well known that in the spectrum of carbonates, the double degenerated v_3 vibration is observed as two bands in the infrared [35]. Busca and Lorenzelli [32] proposed the use of the magnitude of the split of these two bands to distinguish the different species of carbonates.
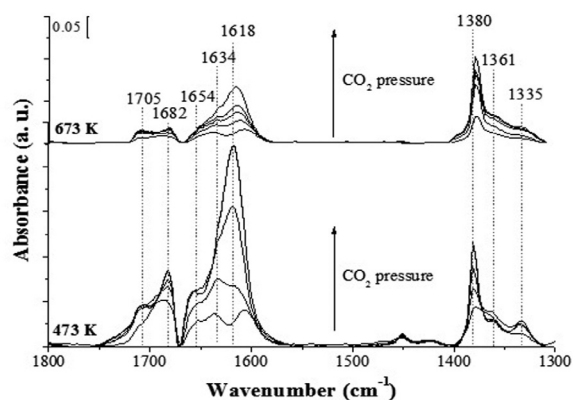

Fig. 1. XRD diffractograms of prepared samples.

Fig. 2. N_2 adsorption-desorption isotherms.

Fig. 3. IR spectra of Na-MOR activated at 473 K (bottom) and 673 K (top) contacted for 30 min with measured amounts of CO_2 (~26, 66, 100, 110 and 130μmol). The IR spectra were obtained after subtracting the contributions of the gas phase and the clean surface.

When Na-MOR is activated at 473 K, the contact with ~26 µmol of CO_2 gives rise to a spectrum with clear maxima at 1682, 1634 and 1606 cm^{-1}, and shoulders at 1705 and 1654 cm^{-1}. With increasing CO_2 pressures, the bands at 1705, 1654, 1361 and 1335 cm^{-1} are better defined and the band at 1606 shifts to 1618 cm^{-1}. Also, bands are observed at 1454 and 1423 cm^{-1}.

The bands at 1454 and 1423 cm^{-1} arise from monodentate carbonates since they are observed in the corresponding region and have a small Δv_3 (31 cm^{-1}) [10,14,22], that according to Busca *et. al.* [23] correspond to this type of carbonate.

The bands at 1654, 1634 and 1618 cm^{-1} along with the bands at 1361 and 1335 cm^{-1} could be assigned to bidentate carbonates [13,14,36-38]. However, the main band of bicarbonate can be observed in the same zone (~1620 cm^{-1}) [39]. The analysis of the variations in absorbance with the CO_2 pressure can help to distinguish between these two species. The bands at 1654, 1634 cm^{-1} and 1361, 1335 cm^{-1} show a slight intensity increase with the CO_2 pressure while the intensity increment of the band at 1618 cm^{-1} is large. Besides, the Δv_3 of the two doublets at 1654-1361 cm^{-1} and 1634-1335 cm^{-1} is 296 cm^{-1}, which according to Busca *et. al.* [32] correspond to bidentate carbonates. Therefore, the band at 1618 cm^{-1} is assigned to bicarbonates while the bands at 1654, 1634 cm^{-1} and 1361, 1335 cm^{-1} are assigned to the high and low frequency of the v_3 vibration of bidentate carbonates, respectively. Further discussion about the assignation of these bands will be presented in the following sections.

Finally, the bands at 1705 and 1682 cm^{-1} can be assigned to polydentate carbonates (also called "bridged bidentate carbonates") [31,40]. In this case the bands at low wave numbers are in the region of the zeolite cut-off.

The spectra of the adsorption of CO_2 on Na-MOR activated at 673 K are also shown in Fig. 3. The absorbance of the bands is smaller due to the dehydration of the zeolite. The bands assigned to monodentate carbonate are no longer present because the formation mechanism of this type of carbonate involves water molecules [16].

The adsorption of CO_2 at higher temperatures produces mainly physisorbed CO_2. When 130 µmol of CO_2 are contacted with Na-MOR at 373, 473, and 573 K, the spectra showed the band at 1380 cm^{-1}, assigned to the symmetric vibration of physisorbed CO_2, in contrast with reported experiments that mention that CO_2 is adsorbed in mordenite only at room temperature [10]. This band decreased with the increase of adsorption temperatures. The bands of carbonates and bicarbonate are not well defined in the spectra obtained at high temperatures and are observed only as small broad features in the 1750-1550 cm^{-1} region.

The results indicate that the contact at room temperature of Na-MOR activated at low temperature (473 K) with CO_2 produce poly, bi and monodentate carbonates along with bicarbonate. When the zeolite is activated at higher temperature (673 K), the monodentate carbonates are not formed. Hereafter, all experiments were performed on mordenites activated at 673 K.

3.3 Formation of bidentate carbonates during CO_2 desorption on Na-MOR

The stability of the carbonates and bicarbonate was explored after the CO_2 adsorption experiment collecting several spectra while evacuating the cell. Fig. 4 shows the spectrum of Na-MOR with gas in the cell (~130µmol), and those taken during desorption. One spectrum was taken at the beginning of evacuation at room temperature, and another after 30 min of vacuum. The zeolite was then heated to 673 K to record a final spectrum.

In the spectrum of Na-MOR with CO_2 in the cell, the main band of physisorbed CO_2 (2361 cm^{-1}, not shown in Fig. 4) has a "cut-off" shape because the concentration of the adsorbed gas is very high. This band is the most intense at the beginning of desorption, indicating that CO_2 is physisorbed at this stage of the experiment. After 30 minutes of vacuum, the absorbance of this band largely decreases but is still observable in the spectrum. This means that CO_2 desorption is a slow process, and that some physisorbed species are still adsorbed on the zeolite.

The evacuation for 30 min gives rise to a large increase in the absorbance of the spectrum in the 1670-1580 cm^{-1} region (see Fig. 4), in accordance with reports for zeolite X [31]. Particularly, the band of bidentate carbonates at 1637 cm^{-1} increases and becomes the main contribution in the spectrum. Contributions of polydentate carbonates and bicarbonates are also observed in the spectrum.

The increase in the absorbance of this band can be explained by a combination of the polarization power of the Na$^+$ cation and the amount of CO_2 physisorbed in Na-MOR. When many molecules of CO_2 are physisorbed (in the adsorption experiments), the interactions with the Na$^+$ cations are weak. However, the decrease in the number of adsorbed CO_2 molecules (while evacuating cell) makes possible the polarization of the CO_2, that is considered the first step in the formation of carbonates [10]. Therefore, the formation of bidentate carbonates is favored by a low concentration of physisorbed CO_2.

Fig. 4 shows that accordingly to literature reports [31,32,41] the only bands remaining after heating the Na-MOR correspond to polydentate carbonates, showing that these species are the most stable.

When Na-MOR was contacted with CO_2 at 373, 473, and 573 K and later evacuated during 30 min at room temperature, the spectra showed small well defined bands in the carbonates and bicarbonate region at 1654, 1634 and 1618 cm^{-1}.

The results presented above evidence that bidentate carbonate formation is enhanced when fewer molecules of CO_2 are adsorbed on the zeolite. Also, that only polydentate carbonates are stable at high temperatures.

3.4 Effect of exchanged cation in the type of carbonates produced

The formation of carbonates and bicarbonate was analyzed for Na-MOR exchanged with cations of different polarizing power: H$^+$, Na$^+$ (Z^+/r^2_{ionic}) = 0.74, K$^+$ (Z^+/r^2_{ionic}) = 0.43, and Ca^{2+} (Z^+/r^2_{ionic}) = 1.54. A zeolite wafer was contacted with 234 µmol of
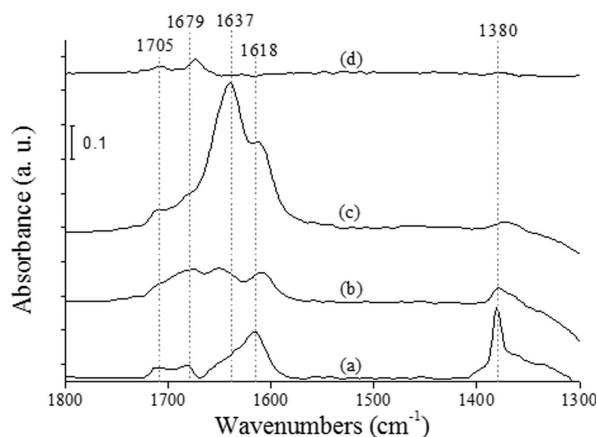
Fig. 4. IR spectra of Na-MOR activated at 673 K. The spectra were collected (a) with ~130 µmol of CO_2 (last dose of CO_2 in the adsorption experiments), (b) at the beginning of evacuation at room temperature ($P=4x10^{-4}$ Torr), (c) after 30 min of vacuum, and (d) after heating the sample to 673 K in vacuum.
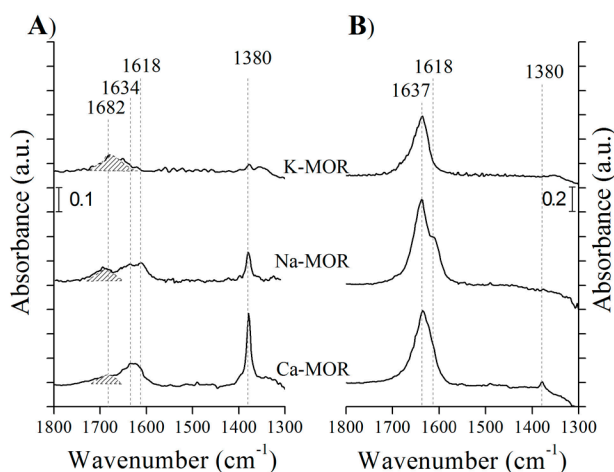
Fig. 5. Infrared spectra collected A) with CO_2 in the cell for 30 min, B) after 30 min of evacuation. (a) Ca-MOR, (b) Na-MOR and (c) K-MOR activated at 673 K.

CO_2 during 30 min, followed by outgassing during 30 min before taking the IR spectra. Figures 5A and 5B show the spectra taken after contacting the wafer with CO_2 for 30 min, and after outgassing 30 min respectively.

The shape of the different spectra indicates that the type of carbonate formed during CO_2 adsorption depends on the exchanged cation. The spectrum of Na-H-MOR (not shown) exhibit smaller bands at the same positions of those of the spectrum of CO_2 adsorbed on Na-MOR described above, shown in Fig. 5A. The amount of chemisorbed and physisorbed species decrease due to the partial exchange of Na^+ with H^+, that do not produce carbonates [42].

The cationic exchange with Ca^{2+}, which has a stronger polarizing power than Na^+ and K^+ due to its smaller size and

higher charge, changes the shape of the spectrum (Fig. 5A). The band of physisorbed CO_2 at 1380 cm^{-1} is more intense, because the Ca^{2+} cations can interact with more CO_2 molecules due to its higher polarizing power. Regarding the carbonate region (1750-1580 cm^{-1}), it is evident that the formation of polydentate carbonates with bands at 1705 and 1682 cm^{-1} is reduced, while the absorbance in the region of bidentate carbonates increases (1654 and 1634 cm^{-1}). The band at 1618 cm^{-1} of bicarbonate slightly decreases.

The exchange with K^+ [43], leads to a weak interaction between CO_2 and the cation (Fig. 5A). Consequently, the band of physisorbed CO_2 is small and bidentate carbonates are not formed. The lack of H^+ in the zeolite, consequence of the full exchange in K-MOR (see Table 1), hinders the formation of bicarbonate. In contrast, the bands of polydentate carbonates are intense in this spectrum.

It appears then that, if mordenite is exchanged with a cation with high polarizing power like Ca^{2+}, the formation of bidentate carbonates will be enhanced, while the exchange with a cation with small polarizing power like K^+, will yield mainly polydentate carbonates. For applications like the elimination of CO_2 from biogas, the use of K-MOR does not seem suitable because surface polydentate carbonates formed on this zeolite are stable even at high temperatures, decreasing therefore the efficiency of the zeolite regeneration process.

After evacuating the CO_2 for 30 min, Fig. 5B shows that the absorbance of all spectra increases. The Na-MOR spectrum displays a very intense bidentate-carbonate band at 1637 cm^{-1} with a clear shoulder arising from bicarbonate at 1618 cm^{-1}. The shape of the band makes evident that the formation of bidentate carbonates is enhanced compared to that of bicarbonates. The spectrum of the partially exchanged Na-H-MOR zeolite (not shown), behaves similarly, but the bidentate carbonate (1637 cm^{-1})/bicarbonate (1618 cm^{-1}) band absorbance ratio changes from 1.8 to 1.4. This indicates a greater presence of bicarbonates due to the presence of H^+ cations in Na-H-MOR [23].In contrast, the spectrum of Ca-MOR shows a single large band at 1635 cm^{-1} arising from bidentate carbonate. In this case, the band of bicarbonate at 1618 cm^{-1} is observed only as an asymmetry.

The spectrum of K-MOR after outgassing, shows, unexpectedly, an intense band of bidentate carbonates at 1636 cm^{-1}, showing that when fewer molecules of CO_2 are in contact with K^+, the cation is able to polarize them despite its low polarizing power, and form bidentate carbonates. The band at 1636 cm^{-1} is not symmetrical showing at high wavenumbers a small contribution of polydentate carbonates. There is no evidence of any contribution at 1618 cm^{-1} associated with the presence of bicarbonates, in agreement with the lack of H^+ in the zeolite.

The spectra recorded after outgassing allows the analysis of the v_3 vibration band of physisorbed CO_2 because under these conditions the signal for this vibration is no longer saturated. In K-MOR, physisorbed CO_2 is observed at 2345 cm^{-1}, which is similar to the observed vibration frequency of CO_2 in the gas phase, indicating a weak interaction with the cation. In contrast, in the spectra of Na-MOR, Na-H-MOR and Ca-MOR

the band shifts 16 cm^{-1} towards higher wavenumbers, appearing at 2361 cm^{-1} due to the stronger interaction of CO_2 with the cation. The fact that the band at 1380 cm^{-1} (ν_1 of physisorbed CO_2) is still evident in the Ca-MOR spectrum (Fig. 5B) indicates the stronger physisorption of CO_2 on this zeolite.

The results indicate that after 30 min outgassing that is just with few CO_2 molecules in contact with the zeolite, the formation of bidentate carbonates is largely enhanced for all the zeolites regardless of the polarizing power of the exchanged cation. Bicarbonates are formed only when H$^+$ cations are present, as in Na-H-MOR, or in the partially exchanged Na-MOR and Ca-MOR (Table 1), where some H$^+$ ions are still likely to be present.

3.5 Formation of carbonates in hydrated zeolites

The influence of adsorbed water on the adsorption of CO_2 on zeolites is not well understood. There are some reports indicating that water increases the amount of adsorbed CO_2 due to the formation of bicarbonate species [23] on 13X and 5A zeolites, while in the case of faujasites others report a decrease in the CO_2 adsorption capacity and a slower and more difficult formation of carbonates and bicarbonates [10,19,20]. To investigate the role of water during the adsorption of carbon dioxide on mordenite, a zeolite wafer activated at 673 K was contacted with a 72 µmol of water vapor to obtain a strongly hydroxylated surface. Subsequently, the sample was evacuated for 5 minutes to eliminate the water vapor in the cell and a spectrum was taken. Then, 66 µmol of CO_2 were contacted with the zeolite for 30 min and another IR spectrum was taken. Finally, the gas was evacuated, and the wafer was maintained in vacuum for 30 min before taking the IR spectrum. The experiment was performed with all the zeolite samples, obtaining similar results. The spectra shown in Fig. 6 correspond to Na-MOR: a) after contacting the wafer with CO_2 for 30 min, and b) after 30 min in vacuum.

When CO_2 was contacted with the hydroxylated surface of the zeolite, the ν_3 vibration band of physisorbed CO_2 at 2345
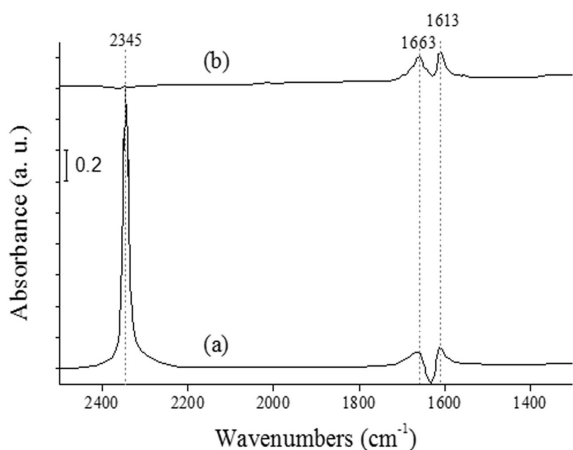
cm^{-1} does not reach saturation, but is still very intense. In contrast in the dehydrated zeolite this band appears in 2361 cm^{-1} and the signal is saturated. Both facts indicate that the presence of water in the zeolite decreases the strength of interaction between the CO_2 and the cation. Moreover, after evacuation of the gas, the band corresponding to physisorbed CO_2 is no longer observed (Fig. 6b). This behavior was similar for all zeolites investigated here and agrees well with the idea that water decreases the CO_2 adsorption capacity of the zeolite.

In the region of carbonates, the IR spectrum of CO_2 contacted with the hydroxylated Na-MOR displays only two small bands at 1663 and 1613 cm^{-1}, that can be assigned to the presence of bicarbonates not interacting with the zeolite because the bands associated with the free HCO_3^- ion are displayed at similar positions [44,45]. No bands of polydentate, bidentate and monodentate carbonates are observed. The bicarbonate bands (Fig. 6) do not increase their absorbance during evacuation, in contrast with the absorbance increase observed in the case of bidentate carbonates (Fig. 5).

In Na-H-MOR, the bicarbonate bands are observed at the same frequency and display the same behavior as for Na-MOR. In the spectra of Ca-MOR and K-MOR, the bicarbonate bands are observed at 1650 and 1610 cm^{-1}. After evacuation, they disappear and instead a broad, intense band of molecularly adsorbed water is observed at 1628 cm^{-1}. This indicates a weak interaction of the bicarbonates with the surface that can be explained because of the presence of layers of adsorbed water molecules, as suggested by Montanari and Wang [12,23].

According to these results, the presence of water in the zeolite weakens the adsorption of CO_2 on the exchanged cations decreasing the adsorption capacity of mordenite. Therefore, a dehydration step is necessary to efficiently adsorb carbon dioxide on mordenite, regardless of the exchanged cation.

For CO_2 adsorption-regeneration applications like biogas cleaning CO_2 physisorption must be favored and this follows the order: Ca-MOR>Na-MOR>K-MOR. The formation of polydentate carbonates, as in K-MOR, must be avoided because its greater stability on the surface hinders the regeneration of the zeolite surface even at temperatures of 400 ºC.

4. Conclusions

- The IR study of the interaction of CO_2 with the surface of mordenite exchanged with Na$^+$, K$^+$ and Ca^{2+} revealed the presence of bicarbonates and several types of carbonates in addition of physisorbed CO_2.
- The distribution of carbonates changed with the polarizing power of the exchanged cation. Mostly bidentate carbonates are produced when the mordenite is exchanged with Ca^{2+}, a cation with high polarizing power. In contrast, mainly polydentate carbonates are formed on mordenite exchanged with potassium, which has the lowest polarizing power.
- The adsorption of CO_2 on sodium mordenite gives rise to mono, bi, and polydentate carbonates, along with bicarbonate. Monodentate carbonate is only formed when the

Fig. 6. IR spectra of surface species arising on Na-MOR hydrated surface (a) after 30 minutes of CO_2 introduction and (b) after 30 min of evacuation.

mordenite is partially dehydrated, because the formation of this species requires the presence of water molecules.

- At low concentrations of CO_2 on the zeolites, a strong inter-action between the CO_2 molecules and the exchanged cations is favored leading to the polarization of the CO_2 molecule, favoring the formation of bidentate carbonates.
- The presence of adsorbed water on the zeolite weakens the physisorption of CO_2 on the cations and produces only bicar-bonates.
- The adsorption of CO_2 on mordenite leads to carbonates with different stabilities related to the type of exchanged cation. This must be taken into consideration for the selec-tion of the exchanged mordenite for adsorption-regenera-tion applications.

Acknowledgments

References

1. C. Da, C. Gomez, The Biogas Handbook, Elsevier, 2013.
2. J. Biswas, R. Chowdhury, P. Bhattacharya, Biomass and Bioener-gy 31 (2007) 80-86.
3. S. Rasi, A. Veijanen, J. Rintala, Energy 32 (2007) 1375-1380.
4. B. Wu, X. Zhang, Y. Xu, D. Bao, S. Zhang, J. Clean. Prod. 101 (2015) 251-261.
5. R. Augelletti, M. Conti, M.C. Annesini, J. Clean. Prod. 140 (2016) 1390-1398.
6. R. V. Siriwardane, M.S. Shen, E.P. Fisher, Energy and Fuels 17 (2003) 571-576.
7. Y. Cheng, Q. Huang, M. Eić, B.J. Balcom, Langmuir 21 (2005) 4376-4381.
8. E. Finocchio, T. Montanari, G. Garuti, C. Pistarino, F. Federici, M. Cugino, G. Busca, Energy & Fuels 23 (2009) 4156-4159.
9. I. Esteves, M.S.S. Lopes, P.M.C. Nunes, J.P.B. Mota, Sep. Purif. Technol. 62 (2008) 281-296.
10. E. Gallei, G. Stumpf, J. Colloid Interface Sci. 55 (1976) 415-420.
11. J.W. Ward, H.W. Habgood, J. Phys. Chem. 70 (1966) 1178-1182.
12. T. Montanari, G. Busca, Vib. Spectrosc. 46 (2008) 45-51.
13. E.J. Doskocil, R.J. Davis, J. Catal. 188 (1999) 353-364.
14. D. Bonenfant, M. Kharoune, P. Niquette, M. Mimeault, R. Hau-sler, Sci. Technol. Adv. Mater. 9 (2008) 1468-6996.
15. A. V. Larin, Microporous Mesoporous Mater. 200 (2014) 35-45.
16. P.A. Jacobs, F.H. Van Cauwelaert, E.F. Vansant, J. Chem. Soc. Faraday Trans. 69 (1973) 2130.
17. F. Yagi, H. Tsuji, H. Hattori, Microporous Mater. 9 (1997) 237-245.
18. J.C.M. Pires, F.G. Martins, M.C.M. Alvim-Ferraz, M. Simões, Chem. Eng. Res. Des. 89 (2011) 1446-1460.
19. F.A. Cotton, G. Wilkinson, P.L. Gaus, Basic Inorganic Chemistry, 3rd ed., John Wiley & Sons, Inc., 1994.
20. G. Maurin, P. Senet, S. Devautour, F. Henn, J.C. Giuntini, J. Non-Crystallyne Solids 310 (2002) 1050-1054.
21. R. Arletti, L. Gigli, F. di Renzo, S. Quartieri, Microporous Meso-porous Mater. 228 (2016) 248-255.
22. L. Bertsch, H.W. Habgood, J. Phys. Chem. 67 (1963) 1621-1628.
23. Y. Wang, M.D. LeVan, J. Chem. Eng. Data 55 (2010) 3189-3195.
24. C. Baerlocher, L.B. McCusker, D.H. Olson, Atlas of Zeolite Framework Types, 6th ed., Elsevier Ltd., 2007.
25. J.A. Delgado, M. a. Uguina, J.M. Gómez, L. Ortega, Sep. Purif. Technol. 48 (2006) 223-228.
26. [26] Y. Nishimura, H. Takahashi, Kolloid-Z. U. Z. Polym. 245 (1971) 415-419.
27. W.J. Mortier, J. Phys. Chem. 81 (1977) 1334-1338.
28. B.C. Lippens, J.H. de Boer, J. Catal. 4 (1965) 319-323.
29. F. Rouquerol, J. Rouquerol, K. Sing, in:, Adsorpt. by Powders Po-rous Solids, Elsevier, 1999, pp. 219-236.
30. G. Maurin, P. Senet, S. Devautour, P. Gaveau, F. Henn, V.E. Van Doren, J.C. Giuntini, J. Phys. Chem. B 105 (2001) 9157-9161.
31. R.W. Stevens, R. V Siriwardane, J. Logan, Energy and Fuels 22 (2008) 3070-3079.
32. G. Busca, V. Lorenzelli, Mater. Chem. 7 (1982) 89-126.
33. G. Maurin, R.G. Bell, S. Devautour, F. Henn, J.C. Giuntini, J. Phys. Chem. B. 108 (2004) 3739-3745.
34. S. Devautour, A. Abdoulaye, J.C. Giuntini, F. Henn, J. Phys. Chem. B 105 (2001) 9297-9301.
35. J. Fujita, A.E. Martell, K. Nakamoto, J. Chem. Phys. 36 (1962) 339.
36. S.E. Siporin, B.C. McClaine, R.J. Davis, Langmuir 19 (2003) 4707-4713.
37. C. Gensse, T.F. Anderson, J.J. Friplat, (1980) 3562-3567.
38. Q. Liu, A. Mace, Z. Bacsik, J. Sun, A. Laaksonen, N. Hedin, Chem. Commun. 46 (2010) 4502.
39. T. Takaishi, J. Chem. Soc. Faraday Trans. 1 83 (1987) 411.
40. S.K. Wirawan, D. Creaser, Microporous Mesoporous Mater. 91 (2006) 196-205.
41. A. Westermann, B. Azambre, M.C. Bacariza, I. Graca, M.F. Ri-beiro, J.M. Lopes, C. Henriques, Appl. Catal. B Environ. 174-175 (2015) 120-125.
42. C.L. Angell, M. V. Howell, Can. J. Chem. 47 (1969) 3831-3836.
43. S. Peter, J. Sebastian, R. V Jasra, Ind. Eng. Chem. Res. 44 (2005) 6856-6864.
44. J. Baltrusaitis, J.D. Schuttlefield, E. Zeitler, J.H. Jensen, V.H. Grassian, J. Phys. Chem. C 111 (2007) 14870-14880.
45. C. Su, D.L. Suarez. Clays Clay Miner. 45 (1997) 814-825.